

Water Eutrophication based on Multilevel Grid

Amare Charun*

University of Balochistan, Pakistan

**corresponding author*

Keywords: Multi Level Grid, Water Eutrophication, Grid Spatial Database, Grid Construction Method

Abstract: With the acceleration of the process of lacustrization, the ensuing eutrophication disaster of water body has an increasing impact on people's normal life and production. Lake water body calculation model is an important means to realize the mechanism analysis, risk assessment and loss calculation of eutrophication disaster. Aiming at the problems and difficulties existing in the research of eutrophication of lake water, this paper introduces the advanced idea of multi-level grid(MLG) of spatial information to solve the above problems, discusses the general idea of MLG construction method of eutrophication of water, proposes the related technologies of grid spatial database, and finally builds a series of analysis and decision-making models based on MLG through the parameter collection and calibration test analysis of MLG experimental model, Provide strong data support for the prevention and control of water eutrophication(VE) disasters.

1. Introduction

The real rapid development of population data grid was in the s of the last century. With the promotion of technology, researchers began to use remote sensing images to obtain land use and coverage data as modeling indicators for population density calculation, and took the lead in applying them in the United States, Britain and other developed countries. The research on population data grid in China also began to develop rapidly in the mid-s, and formed two types of population data grid models. With the development of lakes, using grid technology to improve VE has become a general trend. Therefore, this paper studies and analyzes VE based on MLG.

Many scholars at home and abroad have analyzed the research of VE based on MLG. RP points out that the key process of lake eutrophication is the growth and reproduction of phytoplankton. Therefore, the main way to reveal the formation mechanism of lake eutrophication is to study the relationship between the concentration of nitrogen, phosphorus and other nutrients in water and the primary productivity of phytoplankton. Foreign scientists have done a lot of research on the formation mechanism of lake eutrophication [1]. Mohapatra s R et al. Understand the different

effects of nitrogen, phosphorus concentration and nitrogen to phosphorus ratio on phytoplankton growth and reproduction by studying and proposing the atomic ratio of dissolved nutrients required for phytoplankton growth and reproduction. Later, based on the research results of lake eutrophication mechanism, scientists proposed to control and treat VE by taking controlling the input of exogenous nutrients as the main measure [2]. MaNai 1 et al. Used the grid model to improve the seed propagation algorithm, Zhang Chao et al. Applied the grid to flood disaster risk assessment, and designed a flood loss assessment model based on spatial grid according to the flood coverage and water depth data [3].

In this paper, by analyzing the causes of eutrophication of water body, simulating the process of eutrophication of water body, building a MLG of eutrophication of water body, making full use of limited resources to realize the calculation of rain and flood of lakes, the hydrological parameters in the flow field collected by the MLG of eutrophication of water body are more authentic and more representative in describing the temporal and spatial change laws of rain and flood processes of lakes. Under the condition of the same model principle and method, the lake rain and flood calculation model using the MLG of water body as the calculation unit has higher simulation accuracy, wider application range and more efficient model operation [4-5].

2. Study on VE based on Multi Grid

2.1. Causes of VE

There are many and complex reasons for the eutrophication of landscape water bodies in lakes, but the main causes are as follows: the water quality of water sources is poor: in general, there are three main water sources of landscape water bodies: tap water, river and lake water, and reclaimed water generated after sewage treatment [6]. Most parts of China are in a state of water shortage or serious water shortage. Most rivers and lakes in China are in a state of pollution, with high contents of nitrogen, phosphorus and other nutrients. Therefore, taking rivers and lakes as the source of landscape water will aggravate the eutrophication of landscape water [7]. Point source pollution mainly refers to the untreated sewage discharged into the landscape water body by means of sewage pipes. Endogenous pollution: the deposited sediment is the main endogenous pollution of landscape water. Rotten plants and dead organisms are deposited in the bottom mud after a series of physical and chemical actions. Therefore, the bottom mud of Landscape Lakes contains a large amount of nitrogen, phosphorus and other nutrients. When the water environment changes and the content of nutrients decreases, the nutrients in the sediment will be released, thus supplementing the nutrients in the landscape water body and still eutrophication of the water body; Man made pollution: people throw garbage into the lake at will, pour domestic or industrial waste water and other uncivilized behaviors, as well as cruise ship oil leakage and other problems, will cause pollution to the water body, increase the concentration of nutrients in the water body and promote the eutrophication of the water body [8-9].

2.2. Basic Concept of MLG for VE

The MLG of VE still belongs to the category of geoscience grid in essence, but as a special expansion of spatial information grid, it is not only the spatial discretization method of lake water body, but also the carrier of hydrological, geographical, environmental, social and economic information of the basin. Its spatial distribution characteristics, organizational storage structure and data acquisition methods are closely related to water source calculation. The MLG of VE divides

the basin into different scale grid units according to the hierarchical relationship of Lake confluence, and each level grid corresponds to different stages of the basin confluence process [10]. Based on the spatial distribution characteristics of grids at all levels, the collection and storage of hydrological, geographical, environmental and other information related to the basin can enable each grid unit to comprehensively reflect the spatial heterogeneity of hydrological parameters in the basin.

The proposal and construction of MLG of special spatial information on VE, on the one hand, realizes the integration of multi-source heterogeneous data in the basin, provides the organization and management mode with grid unit as the reference standard for all kinds of hydrological information, improves the utilization rate of resources while eliminating information islands, and provides a strong support for the parameter collection and model construction of lake water body calculation model; On the other hand, it expands the application scope of the idea of spatial information MLG, provides new thematic application achievements, and enriches the connotation and extension of spatial information grid theory [11-12].

2.3. Multi Level Grid Construction of VE

Construction method of MLG of VE according to the basic concept and main content of MLG of VE, this paper designs a construction method of MLG of VE, as shown in Figure 1.

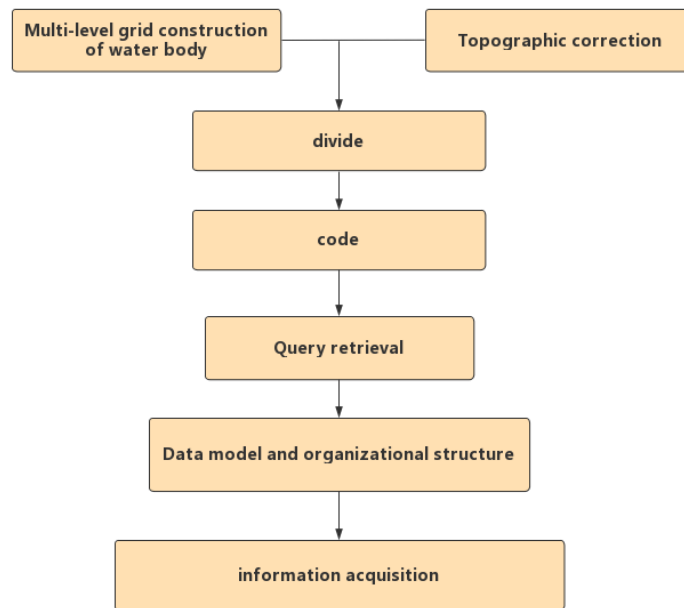


Figure 1. General idea of MLG construction method for eutrophication of water body

This method first combines the characteristics of water production and concentration process to construct a multi-level river network in Huhu Lake Basin, and describes the development process of VE and concentration from macro to micro level. Based on the multi-level river network of the basin, this paper establishes the system structure of MLG of VE, and uses GIS technology to generalize the lake road pipe network system and preprocess the watershed terrain, realizes the

combination of macro and micro concentration systems, and completes the division of grid units at all levels [13-14].

2.3.1. Primary Grid Division and Coding of VE

The primary grid of VE is the confluence interval of the primary river network of the lake basin, which reflects the macro confluence process based on the natural water system of the basin and realizes the overall description of the surface hydrological characteristics of the lake. According to the calculation unit division method based on the macro confluence system of the lake, the confluence section of the first-class river network is each sub basin in the natural river system. In the extraction process, it is not necessary to consider the impact of the micro confluence of the lake. It can be directly divided according to the flow direction calculation results of the original topography of the lake basin, and the geometric figure distribution of the first-class eutrophication grid of the water body can be obtained. The extracted VE primary grid cells have an irregular geometric structure, forming a one-to-one correspondence with the primary river network of the lake basin. The grid coding form is consistent with the coding scheme of the primary river network of the lake basin, so as to inherit its topological relationship and facilitate the interactive query and retrieval between the MLG and the river network [15-16].

2.3.2. Division and Coding of Eutrophication Secondary Grid of Water Body

The secondary grid of VE is the confluence interval of the secondary river network in the lake basin, which reflects the micro confluence process of the basin based on the eutrophication of water pipe network system (the generalization result of road network). According to the division idea of micro concentration calculation unit in the lake basin, the concentration interval of the secondary river network in the lake basin is the drainage area of each pipe section [17]. This paper combines the division methods based on macro and micro confluence systems through the topographic pretreatment of Lake Basin. The corrected basin data and flow direction calculation results not only have a good physical foundation, but also reflect the micro confluence characteristics of the basin surface. The modified surface flow direction information is combined with the spatial distribution information of the secondary river network in the lake basin, and each secondary river network pipe section is taken as the reference of the river system in the basin, and the idea of natural river sub basin extraction is adopted. According to the number of pipe network connections in the sub watershed of VE primary river network and the number of pipe sections contained therein, each VE primary grid can be refined into multiple secondary grid units to form a one to many tree structure [18].

2.3.3. Three Level Grid Division and Coding of VE

The three-level eutrophication grid is the confluence region of the three-level river network in the lake basin. Since the tertiary river network in the lake basin is each sub pipe section formed by dispersing the secondary river according to the node distribution of the pipe section, the tertiary grid of VE should further refine the secondary grid to reflect the more specific micro runoff process within the secondary grid unit. According to the number of sub pipe sections in the secondary river network, the secondary eutrophication grid of each water body will be refined into multiple tertiary grid units with irregular planar geometry, and form a one-to-one correspondence with each sub pipe section.

3. Related Technologies of Grid Spatial Database

Grid spatial database is the product of the combination of grid technology and spatial database technology. It is the gridding of existing spatial database. The purpose is to centralize the data resources, storage resources and network resources that are widely distributed and stored in heterogeneous databases, and provide a unified access interface for external applications.

Metadata is a series of descriptive information about the gsmg data model, and is a direct mapping relationship between users and the databases of each node. This paper designs three types of metadata: role metadata, node metadata and object metadata. Role metadata is the role type description of each connected user, such as anonymous user, registered user or administrator.

Node metadata is the information description of the node database. Such as the name, IP address, location, database system, remaining space, network status and other attributes of the database server. The system associates users' query, retrieval and storage management of the server according to the IP address.

Object metadata includes object attributes and object associations. It is the description information of database objects, including grid layer, vector layer, attribute table and file. The database object information includes the attribute fields of the data itself and the association information with the grid layer. Object attribute usually refers to the field attribute of the data itself, and object association refers to the relationship between the database object and the database server and the grid layer, which acts as a bridge between the grid layer and the node database.

Among them, the object association information in object metadata describes the corresponding relationship between each data object or file object and node database and grid layer, which is also one of the key research contents of this paper.

The characteristic width of the water body grid cell is closely related to the maximum confluence length. If the basin surface range of the grid cell is generalized as a rectangle equal to the area (s) of the grid cell, its length is the maximum confluence length L_{max} of the basin surface within the grid, and the width is the characteristic width h of the grid cell. The characteristic width of the grid cell satisfies:

$$H = S / L_{max} \quad (1)$$

The area of the grid unit is known, and the calculation method of the maximum confluence length is:

$$L_{max} = \max(K_{p,pout}) \quad (2)$$

Where $K_{p,pout}$ represents the geometric distance from any point P within the range of the point grid cell to the grid outlet $pout$. The point with the largest distance from the water outlet is generally the vertex of the mesh geometry. According to the geometry information of the mesh feature class, the polygon profile is extracted. The projection coordinates (p.x, p.y) of each vertex of the polygon are obtained through projection coordinate transformation. Combined with the projection coordinates (pout.X, pout.Y) of the mesh water outlet node, the distance from each vertex to the water outlet node is calculated by the European distance method:

$$K_{p,pout} = \sqrt{(p.x - pout.x)^2 + (p.y - pout.y)^2} \quad (3)$$

The model uses different methods to calculate the flow yield of permeable and impermeable surfaces in the grid. The calibration of some model parameters also takes the ratio of permeable and

impermeable areas in the grid as an important reference. Therefore, the calculation of the ratio of permeable and impermeable areas in the grid is particularly important in the process of model construction.

4. Experimental Test Analysis

4.1. Model Parameter Acquisition and Calibration

In view of the lack of measured hydrological data in the experimental area, this paper adopts the reference table for model parameter calibration provided in the SWMM model user manual, relies on the advantages of multi-level water grid in information integration and data depth mining, and combines the spatial analysis and statistics method based on GIS and RS platform to complete the collection and calibration of runoff model parameters in the experimental area.

4.2. Acquisition and Calibration Results of Primary Grid Parameters of Water Body

The primary water body grid in the test area only contains one grid element, and its geometric range is the circumscribed polygon of the secondary water body grid set in the test area. The collection and calibration results of the primary grid parameters of the water body represent the overall hydrological characteristics of the whole basin in the test area. The specific values of each parameter field are shown in Table 1:

Table 1. Rainwater primary grid parameter collection and calibration results

Field	Value	Field	Value
Characteristic width (m)	1055.3	Maximum penetration rate (mm/h)	74.6
Average gradient (%)	4.64	Stable infiltration rate (mm/h)	3.42
Impermeable ratio (%)	57	Attenuation coefficient	6

4.3. Acquisition and Calibration Results of Secondary Grid Parameters of Water Body

According to the division results of the secondary grid of the water body in the test area, the whole basin contains a total of rainwater secondary grid units, reflecting the micro concentration process based on the secondary river network section in the test area. The parameter collection and calibration results of each grid unit are shown in Figure 2:

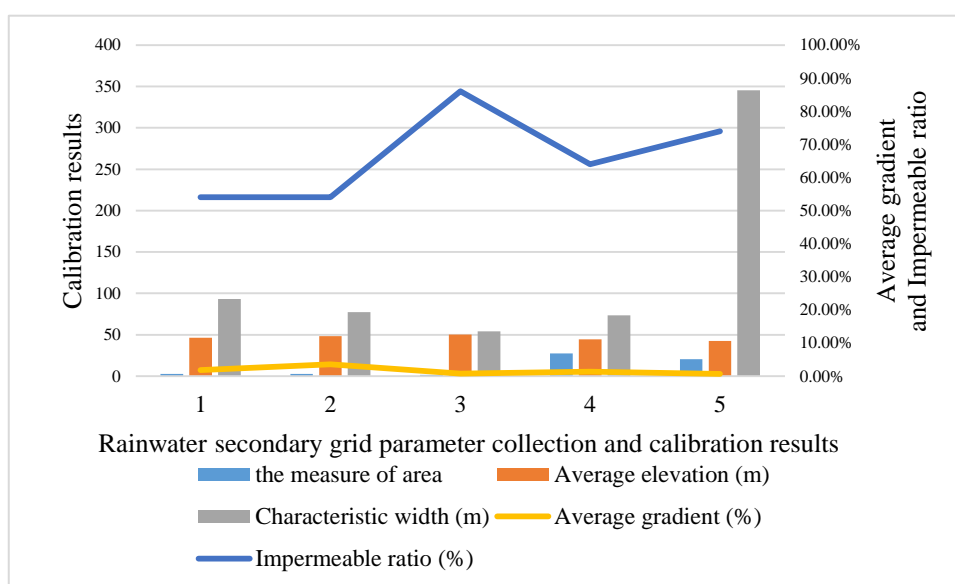


Figure 2. Rainwater secondary grid parameter collection and calibration results

4.4. Water Body Tertiary Grid Parameter Acquisition and Calibration Results

According to the division results of the three-level grid of rainwater in the test area, the whole basin contains three-level grid units of rainwater, reflecting the micro concentration process based on the sub pipe section of the three-level river network in each secondary grid unit. Due to the large number of grid units, only the statistical parameters of each field in the attribute table of grid units are listed here, as shown in Table 2:

Table 2. Rainwater tertiary grid parameter collection and calibration result statistics

Field	Maximum (grid code)	Average value	Minimum (grid coding)
The measure of area	26.45(005S03)	3.49	0.25(007S01)
Average elevation (m)	14.2(023S01)	50.5	36.82(006S01)
Average gradient (%)	368.09(005S03)	2.26	0.2(005S03,016S01)
Characteristic width (m)	100(001S02)	109.5	29.87(007S01)
Impermeable ratio (%)	0.015(001S01)	54.67	0(023S04)

Through the independent sample t-test, it was found that the average pH value of the control group was 9.007, and the average pH value of the heating group was 8.940, which decreased slightly after heating. There was no significant difference between the two ($P = 0.309$), indicating that the heating had little effect on the pH value; The average conductivity of the control group was $217.268 \mu s \cdot cm^{-1}$, and there was a significant difference between the two groups ($P = 0.000$), indicating that increasing the temperature can significantly improve the conductivity of the water

body; The average total phosphorus content of the control group is $0.041\text{mg} \cdot \text{L}^{-1}$, and the average total phosphorus content of the warming group is $0.061\text{mg} \cdot \text{L}^{-1}$. There is a very significant difference ($P = 0.000$) between the two, which indicates that raising the temperature can significantly increase the total phosphorus content in the water body, as shown in Table 3.

Table 3. Physical and chemical indexes of water body (mean value \pm standard error)

	pH	Conductivity ($\mu\text{s cm}^{-1}$)	Dissolved oxygen (mg L^{-1})	Chlorophyll a ($\mu\text{g L}^{-1}$)	Total nitrogen (mg L^{-1})	Total phosphorus (mg L^{-1})
C	9.007 ± 0.046	217.268 ± 2.784	9.426 ± 0.153	2.740 ± 0.196	0.850 ± 0.049	0.041 ± 0.002
T	8.940 ± 0.046	$269.997^{**} \pm 2.853$	$8.429^{**} \pm 0.144$	$4.595^{**} \pm 0.309$	0.852 ± 0.044	$0.061^{**} \pm 0.003$

In the experiment, the change trend of group T and group C was basically the same, which was first stable, then increased, then decreased, and finally remained stable. The possible reason for the early rise is that raising the temperature within a certain range can increase the pH value. When the system is higher than a certain temperature, it will affect other factors in the system, such as slowing down the growth of phytoplankton, weakening the activities of zooplankton and accelerating the decomposition of humus. These factors will reduce the content of carbon dioxide in the water body, resulting in the decline of pH value. The pH value of the control group was 8.528 at the beginning, reaching the highest value of 10.498, and the pH value at the end was 9.325; The pH value of the heating group was 8.527. The results show that increasing temperature will affect the physical and chemical factors of shallow lakes and the community structure of planktonic crustaceans, and affect the recovery of species and the density of planktonic crustaceans. In the experiment, increasing water temperature has different effects on different physical and chemical indexes of water.

5. Conclusion

In this paper, VE is studied based on MLG, and good results are achieved. However, there are still shortcomings: This paper builds a MLG of VE based on the multi-level network system of Lake Basin. When the primary grid of water is refined into a secondary grid, discontinuities may occur. How to consider the impact of the above-mentioned natural water concentration interval on the construction of calculation units is a problem that needs further study. As the MLG of VE and its architecture can reflect the hydrological and physical characteristics of the lake basin, and realize the full integration and utilization of different types of hydrological information from different sources in the basin, the research and application scope of MLG of VE will not be limited to the field of Lake computing. In the future related work, we can further combine the rainwater MLG with various related studies such as Lake disaster loss assessment, emergency decision-making, drainage facility reconstruction and standard formulation, so as to build a series of analysis and decision-making models based on the MLG, and provide strong data support for the prevention and control of VE disasters.

Funding

This article is not supported by any foundation.

Data Availability

Data sharing is not applicable to this article as no new data were created or analysed in this study.

Conflict of Interest

The author states that this article has no conflict of interest.

References

- [1] Rp A, Mb A, Tg A, et al. A techno economic analysis of the power to gas route. *Journal of CO2 Utilization*, 2019, 34(C):616-634. <https://doi.org/10.1016/j.jcou.2019.07.009>
- [2] Mohapatra S R, Agarwal V. Model Predictive Control for Flexible Reduction of Active Power Oscillation in Grid-Tied Multilevel Inverters Under Unbalanced and Distorted Microgrid Conditions. *IEEE Transactions on Industry Applications*, 2020, 56(2):1107-1115. <https://doi.org/10.1109/TIA.2019.2957480>
- [3] Manai L, Hakiri D, Besbes M. Backstepping control of flying capacitor multilevel inverter-based active power filter. *IET Power Electronics*, 2020, 13(19):4610-4624. <https://doi.org/10.1049/iet-pel.2020.0734>
- [4] Kish G J. On the Emerging Class of Non-Isolated Modular Multilevel DC–DC Converters for DC and Hybrid AC–DC Systems. *Smart Grid IEEE Transactions on*, 2019, 10(2):1762-1771.
- [5] Guidi G, D'Arco S, Nishikawa K, et al. Load Balancing of a Modular Multilevel Grid Interface Converter for Transformer-Less Large-Scale Wireless Electric Vehicle Charging Infrastructure. *IEEE Journal of Emerging and Selected Topics in Power Electronics*, 2020, PP(99):1-1.
- [6] Dalu T, Wasserman R J, Magoro M L, et al. River nutrient water and sediment measurements inform on nutrient retention, with implications for eutrophication. *Science of The Total Environment*, 2019, 684(20 Sept):296-302.
- [7] Prasertphon R, Jitchum P, Chaichana R. Water Chemistry, Phytoplankton Diversity And Severe Eutrophication With Detection Of Microcystin Contents In Thai Tropical Urban Ponds. *Applied Ecology and Environmental Research*, 2020, 18(4):5939-5951.
- [8] Jaiswal D, Pandey J. An ecological response index for simultaneous prediction of eutrophication and metal pollution in large rivers. *Water Research*, 2019, 161(SEP.15):423-438. <https://doi.org/10.1016/j.watres.2019.06.030>
- [9] Larico A, Medina S. Application of WASP model for assessment of water quality for eutrophication control for a reservoir in the Peruvian Andes. *Lakes & Reservoirs*, 2019, 24(1):37-47. <https://doi.org/10.1111/lre.12256>
- [10] Hassan M H, Stanton R, Secora J, et al. Ultrafast Removal of Phosphate from Eutrophic Waters Using a Cerium-Based Metal–Organic Framework. *ACS Applied Materials And Interfaces*, 2020, 12(47):52788-52796. <https://doi.org/10.1021/acsami.0c16477>
- [11] Hussein R M, Sen B, Sonmez F. Eutrophication Process and Water Quality Indices. *International Journal of Engineering Technologies and Management Research*, 2020, 6(9):76-83.
- [12] Pierzchaa U. Assessment of the possibility of using remote sensing methods for measuring eutrophication of inland water reservoirs. *Inżynieria Ekologiczna*, 2020, 21(4):27-32. <https://doi.org/10.12912/23920629/129586>
- [13] Jahan H K, Abapour M. Switched-Capacitor-Based Multilevel Inverter for Grid-Connected

- Photovoltaic Application. IEEE Transactions on Power Electronics, 2020, PP(99):1-1.*
- [14] Bougarne L, Abbou M B, Haji M E, et al. *Consequences of surface VE: remedy and environmental interest. Materials Today: Proceedings, 2019, 13(12):654-662. <https://doi.org/10.1016/j.matpr.2019.04.025>*
- [15] Chamarthi P, Al-Durra A, El-Fouly T, et al. *A Novel Three-Phase Transformerless Cascaded Multilevel Inverter Topology for Grid-Connected Solar PV Applications. IEEE Transactions on Industry Applications, 2020, PP(99):1-1.*
- [16] Raudsepp U, Maljutenko I, Kouts M, et al. *Shipborne nutrient dynamics and impact on the eutrophication in the Baltic Sea. The Science of the Total Environment, 2019, 671(JUN.25):189-207.*
- [17] Chetia R, Sawasdee V, Popradit A, et al. *Alteration of Spatial Pollution Compounds to Eutrophication Phenomenon of Small-Scale Area under Corona Virus Disease Circumstances. Journal of Environmental Management and Tourism, 2020, 12(3(51)):613-620. [https://doi.org/10.14505/jemt.v12.3\(51\).01](https://doi.org/10.14505/jemt.v12.3(51).01)*
- [18] Derolez V, Bec B, Munaron D, et al. *Recovery trajectories following the reduction of urban nutrient inputs along the eutrophication gradient in French Mediterranean lagoons. Ocean & Coastal Management, 2019, 171(APR.):1-10. <https://doi.org/10.1016/j.ocecoaman.2019.01.012>*